HHS Public Access

Author manuscript

Ophthalmol Retina. Author manuscript; available in PMC 2022 May 01.

Published in final edited form as:

Ophthalmol Retina. 2021 May ; 5(5): 396–408. doi:10.1016/j.oret.2020.12.010.

Local anatomic precursors to new onset geographic atrophy in age-related macular degeneration as defined on optical coherence tomography

Malini Veerappan Pasricha, MD[1,2], **Vincent Tai, MS**[1], **Karim Sleiman, MD**[1,3], **Katrina Winter, BS**[1], **Stephanie J Chiu, PhD**[1], **Sina Farsiu, PhD**[1,4], **Sandra S Stinnett, DPH**[1], **Eleonora M Lad, MD PhD**[1], **Wai T Wong, MD**[5], **Emily Y Chew, MD**[5], **Cynthia A Toth, MD**[1,4] **for the Age-related Eye Disease Study 2 Ancillary Spectral Domain Optical Coherence Tomography Study Group**

[1]Duke Eye Center, Duke University Medical Center, Durham, NC

[2]Byers Eye Institute, Stanford University Medical Center, Palo Alto, CA

[3]The Statistical Consulting Center, Maa Data Group, Beirut, Lebanon

[4]Department of Biomedical Engineering, The Pratt School of Engineering, Duke University, Durham, NC

[5]National Eye Institute, National Institute of Health, Bethesda, MD

Abstract

Purpose: In macula-wide analyses, spectral domain optical coherence tomography (SDOCT) features such as drusen volume, hyperreflective foci and OCT-reflective drusen substructures independently predict onset of geographic atrophy (GA) secondary to age-related macular degeneration (AMD). We sought to identify SDOCT features in the location of new GA prior to its onset.

Design: Retrospective study

Subjects: Age-Related Eye Disease Study 2 Ancillary SDOCT Study Participants

Methods: We analyzed longitudinally-captured SDOCT and color photographs from 488 eyes (of 488 participants) with intermediate AMD at baseline. Sixty-two eyes with sufficient image quality demonstrated new onset GA on color photographs during study years two through seven. The area of new onset GA and one size-matched control region in the same eye were separately segmented and corresponding spatial volumes on registered SDOCT images at the GA incident year, and at two, three, and four years prior were defined. Differences in SDOCT features between paired precursor regions were evaluated through matched-pairs analyses.

Correspondence: Cynthia A. Toth. Duke Eye Center, Duke University Medical Center, 2351 Erwin Road- Box 3802, Durham, NC 27710. cynthia.toth@duke.edu. Phone: 919-684-0544.

Main outcome measure: Localized SDOCT features two years prior to GA onset

Results: Compared to paired control regions, GA precursor regions at two, three and four years prior (n=54, 33 and 25, respectively) had greater drusen volume (p=0.01, p=0.003 and p=0.003 respectively). At two and three years prior to GA onset, they were associated with the presence of hypertransmission (p<0.001 and p=0.03), hyperreflective foci (p<0.001 and p=0.045), OCT-reflective drusen substructures (p=0.004 and p=0.03), and loss/disruption of: photoreceptor zone, ellipsoid zone, and retinal pigment epithelium (two-year p<0.001 and three-year p=0.005–0.045). At four years prior, precursor regions were associated with photoreceptor zone thinning (p=0.007) and interdigitation zone loss (p=0.045).

Conclusions: Evolution to GA is heralded by early local photoreceptor changes and drusen accumulation, detectable 4 years prior to GA. These precede other anatomical heralds such as RPE changes and drusen substructure emergence detectable 1–2 years prior to GA. This study thus identifies earlier endpoints for GA as potential therapeutic targets in clinical trials.

Precis

Localized SDOCT-based features preceding onset of geographic atrophy in age-related macular degeneration are greater drusen volume, disruption of outer retinal layers, hyperreflective foci above drusen and OCT-reflective substructures within drusen.

Geographic atrophy (GA) is a hallmark feature of late nonexudative age-related macular degeneration (AMD), the leading cause of irreversible blindness in adults over the age of 65 in developed countries.[1–3] Structural biomarkers that can improve the prediction of progression to GA will be useful in identifying patients at risk for vision loss from AMD.[4]

Precursors to GA on color photographs (CP) have been previously reported. In a 15-year population based prospective study, Klein et al. described localized changes in the retina prior to new onset of GA as large drusen and hyperpigmentation, followed by drusen regression and hypopigmentation, then by GA.[5] In another retrospective cohort study of 89 eyes, most cases of GA (84%) formed in areas previously occupied by drusen.[6] Specifically, 35% were preceded by soft confluent drusen, 33% by drusenoid pigment epithelial detachments, 12% by calcified drusen, and 4% by a combination of drusen types in multifocal GA.[6] However, evaluation of detailed retinal features that precede GA beyond drusen and pigmentation is limited on CP. Furthermore, precise measurement of drusen volume and rate of change is not possible on CP.

Spectral domain optical coherence tomography (SDOCT) provides reflectance-based cross-sectional visualization of drusen and retinal structures at high (<5 μm) axial resolution.[7] In macula-wide assessments, several groups including ours have reported features on SDOCT, such as drusen area, drusen volume, subfoveal choroidal thickness, outer retinal tubulation, hyperreflective foci (HRF), subretinal drusenoid deposits and OCT-reflective drusen substructures (ODS), that predict progression to GA or enlargement of GA.[8–17] We were interested to investigate a larger repertoire of SDOCT features that may focally precede development of GA and sought to quantify these features. We hypothesized that abnormally high or low drusen volumes, SDOCT features of HRF and ODS, as well as disruption in the photoreceptor and RPE layers may confer risk of localized GA progression. In this study,

we evaluate the range of features and the timeline of their onset on SDOCT as they focally precede new onset GA in intermediate AMD eyes from the prospective Age Related Eye Disease Study 2 (AREDS2) Ancillary SDOCT Study.

METHODS

Participants were AMD patients enrolled in the prospective, interventional Age-Related Eye Disease Study 2 (AREDS2, ClinicalTrials.gov identifier NCT00345176) and consented to participate in the AREDS2 Ancillary SDOCT Study (A2A SDOCT Study, ClinicalTrials.gov identifier NCT00734487). The study was approved by the Institutional Review Board (IRB) at each of 4 clinical sites. Informed written consent was obtained prior to enrollment from each study participant, and the research protocol followed tenets of human research as presented in the Declaration of Helsinki. Data were collected, stored, and managed in compliance with Health Insurance Portability and Accountability Act guidelines.

Study Design and Procedures

The A2A SDOCT study design was described previously.[18] Participating sites recruited 349 participants between 50 and 85 years of age with at least one eye with large drusen without central GA or AREDS2-determined choroidal neovascularization. At baseline and each annual study visit, each participant had AREDS2 CPs and A2A SDOCT Study imaging (100 SDOCT B-scans with 1000 A-Scans per B-scan across a 6.7 by 6.7 mm region) using the Bioptigen Tabletop SD-OCT system (Research Triangle Park, NC). Areas of GA were determined on CP by two graders (MVP and EML, arbitrated by CAT in cases of disagreement), using the Wisconsin Reading Center GA definition of “an area of partial or complete depigmentation of the RPE within the macula that is circular ≥433 μm in diameter, with at least two of the following three features: roughly round or oval in shape, sharp margins, and visible underlying choroidal vessels.”[19]

At the time of baseline imaging in the A2A Study, 33 participants were excluded for bilateral advanced AMD on SDOCT. Among the 488 eligible eyes from the remaining 316 participants, 411 eyes had no GA at baseline and were therefore determined at risk of developing GA during the follow-up years. Eighty-three eyes developed new onset GA in follow-up years; 10 were excluded because they were from participants already contributing a study eye (right eye arbitrarily chosen) and 11 were excluded for poor SDOCT scan quality, leaving 62 eyes of 62 participants analyzed in this study (Figure 1). We did not differentiate between patients who were in the intervention vs. sham group in the original AREDS2 study.

Within eyes with new onset GA, graders used the proprietary software Duke OCT Retinal Analysis Program (DOCTRAP) Version 61.4.2 (MATLAB R2012a, Mathworks, Natick, Massachusetts) to mark regions of interest (ROI) on the CP. The GA ROI was a circular area of diameter adequate to encircle the margin of an individual region of new onset GA, one per eye. In the same eye, a circular control ROI of equal diameter and approximate distance from the foveal center, which could contain drusen, pigmentation, and/or normal-appearing retina but not GA, was marked for comparison. The choice between multiple possible control regions that fulfilled these criteria was arbitrary, though the furthest possible region

from the GA area was prioritized. Using the DOCTRAP software, each GA and control ROI pair was registered from CP to the corresponding location on SDOCT at GA incident year *t*, and then from SDOCT year onto the corresponding location at years t − 2, t − 3, and t − 4. Manual marking of the foveal center and optic nerve head on CP was required for image registration. Two years prior to GA onset (t − 2) was our primary timepoint. Upon completion of the analysis, we recognized that one year prior to GA and incident year of GA would also be valuable, and therefore added year t − 1 and year t to the retinal layer volume analysis.

The SDOCT scans through each GA precursor and matched control ROI were evaluated by a grader masked to the ROI designation and year of the visit. Among the outcomes measured were the following retinal volume measurements: RPE Drusen Complex (RPEDC) volume (defined as combined volume of drusen and RPE) volume, RPEDC Abnormal Thickening volume, RPEDC Abnormal Thinning (RAT) volume, Neurosensory Retinal (NSR) volume.[12,13,20] The outcomes measured also included the following SDOCT features of the retina and RPE: RPE Elevation, external limiting membrane disruption, photoreceptor zone thinning, ellipsoid zone loss/disruption, interdigitation zone loss/disruption, RPE layer loss/disruption, hypertransmission,[21] vitreomacular traction/epiretinal membrane, cystoid spaces, subretinal fluid, subretinal or intraretinal lesion (individual lesion types reported separately in results section), Hyperreflective Foci (HRF), and OCT-reflective Drusen Substructures (ODS). These study outcomes are detailed in Table 1.[12,13,20,22,23] The results for each GA precursor ROI were compared to those in its corresponding control ROI at the same precursor year. For individual ROIs whose limits extended beyond the 5 mm diameter macular region, we calculated partial retinal volumes for the portion of the ROI that was within bounds. Similarly, for the qualitative grading of AMD-related features of the retina and RPE, ROIs whose limits extended beyond the 6.7×6.7mm SDOCT scanning field under consideration were graded in partiality for any portion of the region within bounds.

Data Analysis

At each precursor year, we compared continuous and categorical outcomes within GA ROIs to those within paired control ROIs. Retinal volume measurements were continuous outcomes and were standardized by dividing by the ROI area (which varied across each GA-control pair). Continuous outcomes were compared using the Wilcoxon Signed Rank Test for matched pairs. Categorical variables were AMD-disease features primarily graded as present or absent and were compared using the Bowker's Test for matched pairs.

RESULTS

Sixty-two eyes had new onset GA on CP and corresponding SDOCT volumes at GA incident year. ROI diameters ranged from 0.41 mm to 3.78 mm (mean 1.07 ± 0.59 mm). At precursor years t − 1, t − 2, t − 3 and t − 4, there were 53, 54, 33 and 25 eyes, respectively, with one GA and one corresponding control ROI registered per SDOCT volume.

Two-Year Precursor Regions

Analysis of precursor regions with respect to future GA presence or absence is shown in Table 2. Regions two years prior to GA onset were associated with higher RPEDC volume (mean: 0.0381 mm^3 GA vs. 0.0320 mm^3 No GA, p=0.01), but not with RPEDC Abnormal Thickening, RAT, or NSR volumes. Two-year GA precursor regions were also associated with photoreceptor zone thinning (66.7% GA vs. 24.1% No GA, p<0.001), ellipsoid zone loss (98.2% GA vs. 77.8% No GA, p<0.001), RPE layer loss (98.2% GA vs. 42.6% No GA, p<0.001), hypertransmission (68.5% vs. 20.4%, p<0.001), and a trend toward external limiting membrane disruption (95.6% GA vs. 84.4% No GA, p=0.059). Though a paired statistical analysis could not be conducted due to asymmetric data, 2-year GA precursor regions had a higher proportion of RPE elevation (100% GA vs. 81.5% No GA), interdigitation zone loss (100% GA vs. 94.0% No GA), and subretinal fluid (7.4% GA vs. 0.0% No GA). Interestingly, 2-year precursor regions were associated with a lower proportion of subretinal lesions (9.3% GA vs. 27.8% No GA, p=0.004), which were predominantly subretinal drusenoid deposits in the control group (Table 3). With regard to special SDOCT features, 2-year GA precursor regions were associated with HRF (55.6% GA vs. 20.4% No GA, p<0.001) and ODS (31.8% GA vs. 4.6% No GA, p=0.003). While we report photoreceptor zone thinning, RPE layer loss, and hypertransmission as binary variables, these outcomes were also given rank scores to provide a more detailed characterization of these features (Table 4).

Three-Year Precursor Regions

Regions three years prior to GA onset (Table 2) were associated with higher RPEDC volume (mean: 0.0408 mm^3 GA vs. 0.0319 mm^3 No GA, p=0.003), but not with greater RPEDC Abnormal Thickening, RAT, or NSR volumes. Three-year GA precursor regions were also associated with RPE elevation (i.e. drusen or pigment epithelial detachments, 97.0% GA vs. 84.9% No GA, p=0.045), external limiting membrane disruption (95.5% GA vs. 77.3% No GA, p=0.045), photoreceptor zone thinning (54.6% GA vs. 27.3% No GA, p=0.01), ellipsoid zone loss (90.6% GA vs. 65.6% No GA, p=0.01), RPE layer loss (81.8% vs. 42.4%, p=0.005), and hypertransmission (48.5% GA vs. 24.2% No GA). Though a paired statistical analysis could not be conducted due to asymmetrical data, 3-year GA precursor regions had a higher proportion of subretinal fluid (6.1% GA vs. 0.0% No GA). Additionally, 3-year GA precursor regions were associated with a higher proportion of cystoid spaces (25.0% GA vs. 6.3% No GA, p=0.03), which were found as single, isolated features in each region (Table 3). With regard to special SDOCT features, 3-year GA precursor regions were associated with HRF (42.4% GA vs. 18.2% No GA, p=0.045) and with ODS (21.4% GA vs. 3.6% No GA, p=0.03). Rank scores were also compared between 3-year GA precursor regions versus control regions (Table 4).

Four-Year Precursor Regions

Regions four years prior to GA onset (Table 2) were associated with higher RPEDC volume (mean: 0.0482 mm^3 GA vs. 0.0388 mm^3 No GA, p=0.003), higher RPEDC Abnormal Thickening volume (mean: 0.5470 mm^3 GA vs. 0.0378 mm^3 No GA, p=0.02), and lower RAT volume (mean: 0.6000 mm^3 GA vs. 1.270 mm^3 No GA, p=0.04), but not with

difference in NSR. Four-year GA precursor regions were also associated with photoreceptor zone thinning (48.0% GA vs. 12.0% No GA, p=0.003) and interdigitation zone loss (96.0% GA vs. 80.0% No GA, p=0.045). The 4-year GA precursor regions had a higher proportion of RPE elevation (100% GA vs. 84.0% No GA) and subretinal fluid (4.2% GA vs. 0.0% No GA). With regard to special SDOCT features, 4-year GA precursor regions were associated with a trend towards higher proportion of HRF (44.0% GA vs. 20.0% No GA, p=0.058), but no longer associated with ODS. Rank scores between 4-year GA precursor regions versus control regions are reported in Table 4.

One-Year Precursor and Incident Year Regions (Post Hoc Analysis)

Though mean RPEDC volume decreased as regions approached new onset GA, the observed pattern of persistently thick RPEDC even two years prior to GA elicited questions about the transition point of drusen collapse into area of atrophy. This prompted a post-hoc analysis of continuous variables alone, in regions one year prior to and at the year of new onset GA (Table 5). The results indicate that mean RPEDC volume is lower in one year compared to two year GA precursor regions (mean: 0.0367 mm^3 vs. 0.0381 mm^3, respectively). The difference in mean RPEDC volume in GA compared to paired control regions was no longer statistically significant (mean: 0.0367 mm^3 GA vs. 0.0350 mm^3 No GA, p=0.08). At GA incident year, the mean RPEDC volume was the same as that in the one year precursor regions (mean: 0.0367 mm^3); however, the standard deviation was considerably higher (SD 0.03 vs 0.01). The mean RPEDC volume of GA regions again did not demonstrate a statistically significant difference compared to paired control regions (mean: 0.0367 mm^3 GA vs. 0.0323 mm^3 No GA, p=0.83). Additionally at GA incident year, although volumes of RAT increased in regions with and without GA, the GA regions were associated with higher RAT volume (mean: 0.9316 mm^3 GA vs. 0.8643 mm^3 No GA, p=0.03) and lower NSR volume (mean: 0.2403 mm^3 GA vs. 0.2497 mm^3 No GA, p=0.02) when compared to the non-GA regions.

Change in Retinal Layer Volume Measurements Across All Study Years

Retinal Pigment Epithelial Drusen Complex (RPEDC) Volume—Figures 2a-b provide a graphical representation of the dynamic changes in RPEDC volume across study years. In Figure 2a, we show the mean of RPEDC volume in GA vs. control regions at each study year. Please note the two lines are not for statistical comparison, as this study is a paired analysis of individual values for GA and control regions. Mean RPEDC volume was higher in GA regions than in control regions at all precursor years (except t − 1) and at GA incident year (year t). In GA regions alone, mean RPEDC volume downtrended as eyes progressed from year t − 4 to t − 1 and was relatively stable from year t − 1 to year of GA incidence. Mean RPEDC volume in control regions demonstrated an initial downtrend, then was stable until year of incident GA except at year t − 1 when it transiently increased. Of note, the standard deviation in GA regions was high relative to control regions at GA incident year. In Figure 2b, we plotted the mean of the differences in RPEDC volume between each GA and control region pair (GA minus control) at each study year. At year t − 4, the difference was positive and relatively large; this decreased until year t − 1 and then increased at GA incident year.

RPEDC Abnormal Thinning (RAT) Volume—Figures 2c-d provide a graphical representation of the dynamic changes in RAT volume across study years. In Figure 2c, we compared the mean of RAT in GA vs. control regions at each study year. Mean RAT is higher in control regions than in GA regions at all precursor years, though relatively equal at GA incident year (year t). In GA regions alone, mean RAT increased as eyes progressed from year t − 4 to year of GA incidence. Mean RAT in control regions demonstrated fluctuations throughout precursor years, though an overall downtrend to year t. In Figure 2d, we plotted the mean of the differences in RAT between each GA and control region pair (GA minus control) at each study year. The magnitude of difference was largest at years t − 3, when the control regions were significantly thinner than GA regions.

RPEDC Abnormal Thickening Volume—Figures 2e-f provide a graphical representation of the dynamic changes in RPEDC Abnormal Thickening volume across study years. In Figure 2e, we compared the mean of RPEDC Abnormal Thickening volume in GA vs. control regions at each study year. Mean RPEDC Abnormal Thickening volume in GA regions alone demonstrated dynamic changes, with transient upward spikes at year t − 3 and GA incident year (year t). Relatively, mean RPEDC Abnormal Thickening volume in control regions were stably low. Of note, GA regions demonstrated a large standard deviation at year t − 3 and especially at GA incident year. In Figure 2f, we plotted the mean of the differences in RPEDC Abnormal Thickening volumes between each GA and control region pair (GA minus control) at each study year. The value fluctuated with the largest differences in year t − 3 and GA incident year.

Neurosensory Retinal (NSR) Volume—Figures 2g-h provide a graphical representation of the dynamic changes in NSR volume across study years. In Figure 2g, we compared the mean of NSR volume in GA vs. control regions at each study year. Mean NSR was higher in control regions than in GA regions at all years, including GA incident year (year t). In GA regions alone, mean NSR downtrended as eyes progressed from year t − 4 to t − 1, when it uptrended before falling at year of GA incidence. Mean NSR in control regions demonstrated a similar trend. In Figure 2h, we plotted the mean of the differences in NSR between each GA and control region pair (GA minus control) at each study year. The difference between paired regions was largest at year t − 1 and GA incident year.

DISCUSSION

We investigated a large selection of independent SDOCT features as localized precursors to new onset GA across a large population. Higher RPEDC volume preceded new onset GA across all precursor years. In the post hoc analysis, though not statistically significant, mean RPEDC volume continued to be higher in GA regions one year prior to GA onset and at GA incident year. The latter demonstrates that higher RPEDC volumes may co-exist with onset of GA, as opposed to demonstrating complete collapse. Furthermore, at GA incident year, though the mean RPEDC volume in GA regions had stabilized, their standard deviation was significantly larger. This may indicate a dynamic, highly variable drusen landscape that occurs in regions of new GA onset. Interestingly, though not statistically significant at every year, RAT volume (defined as volume of RPEDC abnormal thinning ≤2 SD from the mean of a normative dataset for each pixel location in non-AMD eyes)

was higher in control regions than in GA regions at all precursor years, which may indicate that abnormal thinning is not a localized but a generalized change in GA-destined eyes. RAT volume was significantly higher in GA regions compared to control regions at GA incident year. The volume of RPEDC Abnormal Thickening (defined as volume of RPEDC abnormal thickening ≥3 SD from the mean of a normative dataset for each pixel location in non-AMD eyes) were not significantly different in GA versus control regions, except at year − 4 when RPEDC Abnormal Thickening volume was higher in GA regions. The RPEDC Abnormal Thickening volume in GA regions demonstrated significant fluctuation in mean values throughout precursor years, compared to relative stability in control regions, indicating a highly tumultuous RPE environment. RPEDC Abnormal Thickening volume was also notably higher in GA regions compared to control regions at GA incident year, and with a large standard deviation, indicating co-existence of RPE thickening and thinning in regions of GA. Figure 3 demonstrates the findings of RPEDC thickening and thinning on color photograph, SDOCT, and SDOCT-derived thickness maps. Lastly, NSR volume was consistently lower in GA regions compared to paired control regions, though this was only significant at the GA incident year. Taken together with the other retinal layer volume measurements, this highlights that while GA and GA precursor regions consistently demonstrate progressive thinning of the neurosensory retina, measurement of RPE abnormal thinning and thickening in these regions are highly variable and largely co-existent. The dynamism in RPE volumes is supported by prior histopathological studies which demonstrate rounding, stacking, and anterior migration of the RPE layer and thickening of basal laminar deposits in pre-GA regions.[24–29]

The external limiting membrane, photoreceptor zone, ellipsoid zone, interdigitation zone and RPE were all disrupted, lost, or thinned two years prior to GA onset, with associated increase in choroidal signal, compared to control regions. At three years prior to GA onset, we found that all of the retinal layer associations, except interdigitation zone loss, persisted. At four years prior to GA onset, photoreceptor zone thinning and interdigitation zone loss were significant. The progressive loss of retinal layers across precursor years demonstrates a plausible order in deterioration of layers as a retina region develops GA: first, the area begins to lose the photoreceptor zone and interdigitation zone, followed by loss of the external limiting membrane, ellipsoid zone and RPE, and with hypertransmission as a later finding.

With regard to other OCT features, 3-year precursor regions had a higher proportion of cystoid spaces. These cystoid spaces were found as single, isolated entities in each region. We speculate that these “holes” are retinal pseudocysts, described in a previous study as empty spaces with no obvious wall, frequently within the inner nuclear layer and not associated with vitreoretinal traction, macular edema, or choroidal neovascularization.[30] The study reported the presence of pseudocysts in a cross-sectional analysis of eyes with GA, and it is conceivable that these features appear at an earlier stage prior to localized onset of GA, as we have found. It has been speculated that retinal pseudocysts correspond to early loss of Muller cells and/or degenerative gliosis in atrophy pathogenesis.[30,31] Two-year precursor regions also had a higher proportion of cystoid spaces though the difference was no longer statistically significant. We speculate that this is because the early changes in Muller cells has transitioned to more severe loss and atrophy at this stage. Additionally, 2-

year precursor regions interestingly had a lower proportion of subretinal lesions than control regions in the same eye. The majority of the subretinal lesions were subretinal drusenoid deposit (Table 5). Several studies have demonstrated an association between subretinal drusenoid deposit and both forms of late-stage AMD, neovascular and atrophic.[32–34] Our findings show a relatively large number of subretinal drusenoid deposits in both GA and control regions, indicating that they may be a macula-wide feature of pre-GA eyes rather than a regional one. In contrast, Marsiglia et al. demonstrated a spatial association between GA and reticular pseudrusen; specifically, incipient GA progressed significantly more often towards areas previously manifesting subretinal drusenoid deposit.[35] Further studies are needed to determine whether subretinal drusenoid deposit may have a consistent localized effect on progression to GA.

Lastly, with regard to special OCT features, 2- and 3-year precursor regions had a higher proportion of both ODS and HRF. Neither were significant in 4-year precursors regions, though HRF demonstrated a trend. As corroborated by our previous studies and others, HRF and ODS are highly predictive of progression to GA.[13,14,36] This analysis shows further that they occur in the region of GA, and at a time point two to three years prior to the onset of GA.

While conventionally characterized on CP, localized precursors to GA have also been studied on fundus autofluorescence and microperimetry. [37–47] More recently, there has been heightened investigation of localized precursors to GA on SDOCT.[21,48] Guymer et al has shown in several studies that nascent GA, which is defined as the subsidence of the outer plexiform layer and inner nuclear layer and development of a hyporeflective wedge-shaped band within the limits of the outer plexiform layer, is a strong predictor for development of GA.[49,50] In other studies based on SDOCT, heterogenous internal reflectivity of a drusenoid lesion and hyperreflective foci were found to be predictive of local atrophy onset, similar to the findings in our study. [16,36,51,52]

Study limitations included fewer number of regions in earlier precursor years. Additionally, due to our custom image registration program, we were required to use ROIs that were circular in shape and therefore could not trace the exact contour of GA in this study. This also disallowed us to comment on the size of incident GA. Some ROIs were partial due to the 6.7×6.7mm limitation of the SDOCT scanning field; thus, some features present out-of-bounds may have been missed. Lastly, registration of ROIs from CP to OCT, and subsequently from OCT incident year to OCT precursor year, may have introduced error due to varying orientations of SDOCT volumes for the same subject across different years, location limitations due to fixed B-scan increments, and manual marking of foveae and optic nerve heads (required for image registration) on CPs. A broader limitation of the study was that our patients were selected from the aggregate group of AREDS2 participants; we did not differentiate between patients who included the interventional vs. sham groups of the original study. Therefore, it is possible that the natural history of the disease was altered in those participants who were in the intervention group designated to receive the AREDS2 supplement.

Prior studies by our group demonstrated several macula-wide features that predict progression to GA.[12–14] Sleiman et al. created a GA risk assessment model based on the features we identified: hyperreflective foci, RPE layer atrophy/absence, choroid thickness in the absence of subretinal drusenoid deposits, photoreceptor outer segment loss, RPEDC volume, and RAT volume.[53] Similarly, Lei et al. created an OCT-based scoring system based on four OCT features (drusen volume, intraretinal hyperreflective foci, hyporeflective foci within a drusenoid lesion, and subretinal drusen deposits) to predict progression to atrophy and late AMD.[15] Our present study, in contrast, has shown that many of these features occur in the specific region of atrophy itself. It is important to note, however, that these associations are relative rather than absolute. While the significant SDOCT features in this study are associated with GA onset, they may not be necessary for an area to progress to GA. An area without these features may progress to GA. Similarly, as evidenced by some features being present in control regions as well, an area with these features can fail to progress to GA. Without evidence of how many other areas in the eye had these features and what percentage of them progressed to GA, the specific predictive value of these features cannot be determined with the data presented in this study. Lastly, since no one feature was exclusive to GA precursor regions, the individual value of each feature in predicting progression to atrophy is limited. The overall message in the present study is that areas that progressed to atrophy more often had a collection of these specific OCT features compared to areas that did not.

These localized changes likely correspond to biologically active sites in atrophy pathogenesis, as described in several prior studies by Curcio et al.[26–28] Results of this group's studies suggest RPE layer thickening due to cellular dysmorphia and thick basal laminar deposits as precursors to the GA.[24,25] It is plausible that our findings of thickened RPEDC volume in GA precursor regions is correlated with these histopathologic findings. However, we understand that a limitation of this study is our inability to definitively correlate SDOCT findings with histology. Broadly speaking, further studies are needed to address the disconnect between OCT nomenclature and a cellular understanding of disease. In the present study, the co-existence of RPEDC thickening and thinning in regions progressing to GA suggests an early anatomic endpoint for late stage atrophic AMD. A correlation between these features on SDOCT and the molecular pathogenesis of AMD may help us identify therapeutic targets for GA.

Acknowledgments

Financial Support

The Age-Related Eye Disease Study 2 (AREDS2) study was supported by the intramural program funds and contracts from the National Eye Institute of the National Institutes of Health (NIH), Department of Health and Human Services, Bethesda, Maryland (Contract No. HHS-N-260-2005-00007-C. ADB Contract No. N01-EY-5-0007.). The following sponsors supported the AREDS2 Ancillary SDOCT Study and had no role in the design or conduct of this research: Genentech, San Francisco, California (research grant); Alcon, Fort Worth, Texas (research grant); and Bioptigen, Morrisville, North Carolina (research grant).

Conflicts of Interest

Chiu, Farsiu and Toth: Segmentation and identification of layered structures in images- US 20110182517 A1 (patent) Toth: Alcon (royalties), Alcon research grant for this study, Bioptigen research grant for this study, Genentech research grant for this study Veerappan Pasricha (and all other co-authors): None

Appendix

*__Age Related Eye Disease Study 2 (AREDS2) Ancillary SDOCT Study Group__ includes the following: Cynthia A. Toth,[1,2] Wai Wong,[3] Thomas Hwang,[4] G. Baker Hubbard,[5] Sunil Srivastava,[5,6] Michelle McCall,[1] Katrina Winter,[1] Neeru Sarin,[1] Katherine Hall,[3] Patti McCollum,[4] Linda Curtis,[5] Stefanie Schuman,[1] Stephanie J. Chiu,[1] Sina Farsiu,[1] Vincent Tai,[1] Monica Sevilla,[1] Christopher Harrington,[1] Randall Gunther,[1] Du Tran-Viet,[1] Francisco Folgar,[1] Eric Yuan,[1] Traci Clemons,[7] Molly Harrington,[7] Emily Chew[3,8]

[1]Duke Eye Center, [2]AREDS2 Ancillary SDOCT Study Chair, [3]National Eye Institute, [4]Devers Eye Center, [5]Emory Eye Center, [6]Cole Eye Institute, [7]The Emmes Corporation, [8]AREDS2 Chair

Abbreviations/Acroynyms:

GA	geographic atrophy
OCT	optical coherence tomography
SDOCT	spectral domain optical coherence tomography
RPE	retinal pigment epithelium
CP	color photograph
AMD	age-related macular degeneration
AREDS2	Age-Related Eye Disease Study 2
ROI	region of interest
RPEDC	retinal pigment epithelium drusen complex
RAT	RPEDC abnormal thinning
NSR	neurosensory retina
OPL	outer plexiform layer
HRF	hyperreflective foci
ODS	OCT-reflective drusen substructures

REFERENCES

1. Sunness JS, Rubin GS, Applegate CA, et al.Visual function abnormalities and prognosis in eyes with age-related geographic atrophy of the macula and good visual acuity. Ophthalmology. 1997;104(10):1677–1691. [PubMed: 9331210]
2. Tomany SC, Wang JJ, Van Leeuwen R, et al.Risk factors for incident age-related macular degeneration: pooled findings from 3 continents. Ophthalmology. 2004;111(7):1280–1287. [PubMed: 15234127]
3. Klein R, Klein BE, Knudtson MD, Meuer SM, Swift M, Gangnon RE. Fifteen-year cumulative incidence of age-related macular degeneration: the Beaver Dam Eye Study. Ophthalmology. 2007;114(2):253–262. [PubMed: 17270675]

4. Loewenstein A. The significance of early detection of age-related macular degeneration: Richard & Hinda Rosenthal Foundation lecture, The Macula Society 29th annual meeting.Retina (Philadelphia, Pa). 2007;27(7):873–878.
5. Klein ML, Ferris FL 3rd, Armstrong J, et al.Retinal precursors and the development of geographic atrophy in age-related macular degeneration. Ophthalmology. 2008;115(6):1026–1031. [PubMed: 17981333]
6. Brader HS, Ying GS, Martin ER, Maguire MG. Characteristics of incident geographic atrophy in the complications of age-related macular degeneration prevention trial. Ophthalmology. 2013;120(9):1871–1879. [PubMed: 23622873]
7. Khanifar AA, Koreishi AF, Izatt JA, Toth CA. Drusen ultrastructure imaging with spectral domain optical coherence tomography in age-related macular degeneration. Ophthalmology. 2008;115(11):1883–1890. [PubMed: 18722666]
8. Nathoo NA, Or C, Young M, et al.Optical coherence tomography-based measurement of drusen load predicts development of advanced age-related macular degeneration. American journal of ophthalmology. 2014;158(4):757–761.e751.
9. Lee JY, Lee DH, Lee JY, Yoon YH. Correlation between subfoveal choroidal thickness and the severity or progression of nonexudative age-related macular degeneration. Investigative ophthalmology & visual science. 2013;54(12):7812–7818. [PubMed: 24204054]
10. Hariri A, Nittala MG, Sadda SR. Outer retinal tubulation as a predictor of the enlargement amount of geographic atrophy in age-related macular degeneration. Ophthalmology. 2015;122(2):407–413. [PubMed: 25315664]
11. Moussa K, Lee JY, Stinnett SS, Jaffe GJ. Spectral domain optical coherence tomography-determined morphologic predictors of age-related macular degeneration-associated geographic atrophy progression. Retina (Philadelphia, Pa). 2013;33(8):1590–1599.
12. Folgar FA, Yuan EL, Sevilla MB, et al.Drusen Volume and Retinal Pigment Epithelium Abnormal Thinning Volume Predict 2-Year Progression of Age-Related Macular Degeneration. Ophthalmology. 2016;123(1):39–50.e31. [PubMed: 26578448]
13. Christenbury JG, Folgar FA, O'Connell RV, et al.Progression of intermediate age-related macular degeneration with proliferation and inner retinal migration of hyperreflective foci. Ophthalmology. 2013;120(5):1038–1045. [PubMed: 23352193]
14. Veerappan M, El-Hage-Sleiman AM, Tai V, et al.Optical Coherence Tomography Reflective Drusen Substructures Predict Progression to Geographic Atrophy in Age-related Macular Degeneration. Ophthalmology. 2016;123(12):2554–2570. [PubMed: 27793356]
15. Lei J, Balasubramanian S, Abdelfattah NS, Nittala MG, Sadda SR. Proposal of a simple optical coherence tomography-based scoring system for progression of age-related macular degeneration. Graefe's archive for clinical and experimental ophthalmology = Albrecht von Graefes Archiv fur klinische und experimentelle Ophthalmologie. 2017;255(8):1551–1558.
16. Ouyang Y, Heussen FM, Hariri A, Keane PA, Sadda SR. Optical coherence tomography-based observation of the natural history of drusenoid lesion in eyes with dry age-related macular degeneration. Ophthalmology. 2013;120(12):2656–2665. [PubMed: 23830761]
17. Yehoshua Z, Wang F, Rosenfeld PJ, Penha FM, Feuer WJ, Gregori G. Natural history of drusen morphology in age-related macular degeneration using spectral domain optical coherence tomography. Ophthalmology. 2011;118(12):2434–2441. [PubMed: 21724264]
18. Leuschen JN, Schuman SG, Winter KP, et al.Spectral-domain optical coherence tomography characteristics of intermediate age-related macular degeneration. Ophthalmology. 2013;120(1):140–150. [PubMed: 22968145]
19. Davis MD, Gangnon RE, Lee LY, et al.The Age-Related Eye Disease Study severity scale for age-related macular degeneration: AREDS Report No. 17. Archives of ophthalmology (Chicago, Ill : 1960). 2005;123(11):1484–1498.
20. Farsiu S, Chiu SJ, O'Connell RV, et al.Quantitative classification of eyes with and without intermediate age-related macular degeneration using optical coherence tomography. Ophthalmology. 2014;121(1):162–172. [PubMed: 23993787]

21. Sadda SR, Guymer R, Holz FG, et al.Consensus Definition for Atrophy Associated with Age-Related Macular Degeneration on OCT: Classification of Atrophy Report 3. Ophthalmology. 2018;125(4):537–548. [PubMed: 29103793]
22. Chiu SJ, Izatt JA, O'Connell RV, Winter KP, Toth CA, Farsiu S. Validated automatic segmentation of AMD pathology including drusen and geographic atrophy in SD-OCT images. Investigative ophthalmology & visual science. 2012;53(1):53–61. [PubMed: 22039246]
23. Chiu SJ, Li XT, Nicholas P, Toth CA, Izatt JA, Farsiu S. Automatic segmentation of seven retinal layers in SDOCT images congruent with expert manual segmentation. Optics express. 2010;18(18):19413–19428. [PubMed: 20940837]
24. Zanzottera EC, Ach T, Huisingh C, Messinger JD, Freund KB, Curcio CA. VISUALIZING RETINAL PIGMENT EPITHELIUM PHENOTYPES IN THE TRANSITION TO ATROPHY IN NEOVASCULAR AGE-RELATED MACULAR DEGENERATION. Retina (Philadelphia, Pa). 2016;36 Suppl 1(Suppl 1):S26–s39.
25. Dolz-Marco R, Balaratnasingam C, Messinger JD, et al.The Border of Macular Atrophy in Age-Related Macular Degeneration: A Clinicopathologic Correlation. American journal of ophthalmology. 2018;193:166–177. [PubMed: 29981740]
26. Curcio CA, Zanzottera EC, Ach T, Balaratnasingam C, Freund KB. Activated Retinal Pigment Epithelium, an Optical Coherence Tomography Biomarker for Progression in Age-Related Macular Degeneration. Investigative ophthalmology & visual science. 2017;58(6):Bio211-bio226.
27. Li M, Dolz-Marco R, Huisingh C, et al.CLINICOPATHOLOGIC CORRELATION OF GEOGRAPHIC ATROPHY SECONDARY TO AGE-RELATED MACULAR DEGENERATION. Retina (Philadelphia, Pa). 2019;39(4):802–816.
28. Li M, Huisingh C, Messinger J, et al.HISTOLOGY OF GEOGRAPHIC ATROPHY SECONDARY TO AGE-RELATED MACULAR DEGENERATION: A Multilayer Approach. Retina (Philadelphia, Pa). 2018;38(10):1937–1953.
29. Sarks S, Cherepanoff S, Killingsworth M, Sarks J. Relationship of Basal laminar deposit and membranous debris to the clinical presentation of early age-related macular degeneration. Investigative ophthalmology & visual science. 2007;48(3):968–977. [PubMed: 17325134]
30. Cohen SY, Dubois L, Nghiem-Buffet S, et al.Retinal pseudocysts in age-related geographic atrophy. American journal of ophthalmology. 2010;150(2):211–217.e211.
31. Edwards MM, McLeod DS, Bhutto IA, Grebe R, Duffy M, Lutty GA. Subretinal Glial Membranes in Eyes With Geographic Atrophy. Investigative ophthalmology & visual science. 2017;58(3):1352–1367. [PubMed: 28249091]
32. Klein R, Meuer SM, Knudtson MD, Iyengar SK, Klein BE. The epidemiology of retinal reticular drusen. American journal of ophthalmology. 2008;145(2):317–326. [PubMed: 18045568]
33. Pumariega NM, Smith RT, Sohrab MA, Letien V, Souied EH. A prospective study of reticular macular disease. Ophthalmology. 2011;118(8):1619–1625. [PubMed: 21550118]
34. Curcio CA, Messinger JD, Sloan KR, McGwin G, Medeiros NE, Spaide RF. Subretinal drusenoid deposits in non-neovascular age-related macular degeneration: morphology, prevalence, topography, and biogenesis model. Retina (Philadelphia, Pa). 2013;33(2):265–276.
35. Marsiglia M, Boddu S, Bearelly S, et al.Association between geographic atrophy progression and reticular pseudodrusen in eyes with dry age-related macular degeneration. Investigative ophthalmology & visual science. 2013;54(12):7362–7369. [PubMed: 24114542]
36. Tan ACS, Pilgrim MG, Fearn S, et al.Calcified nodules in retinal drusen are associated with disease progression in age-related macular degeneration. Science translational medicine. 2018;10(466).
37. Holz FG, Bellman C, Staudt S, Schutt F, Volcker HE. Fundus autofluorescence and development of geographic atrophy in age-related macular degeneration. Investigative ophthalmology & visual science. 2001;42(5):1051–1056. [PubMed: 11274085]
38. Hartmann KI, Bartsch DU, Cheng L, et al.Scanning laser ophthalmoscope imaging stabilized microperimetry in dry age-related macular degeneration. Retina (Philadelphia, Pa). 2011;31(7):1323–1331.
39. Meleth AD, Mettu P, Agron E, et al.Changes in retinal sensitivity in geographic atrophy progression as measured by microperimetry. Investigative ophthalmology & visual science. 2011;52(2):1119–1126. [PubMed: 20926818]

40. Bearelly S, Cousins SW. Fundus autofluorescence imaging in age-related macular degeneration and geographic atrophy. Advances in experimental medicine and biology. 2010;664:395–402. [PubMed: 20238040]
41. Schmitz-Valckenberg S, Jorzik J, Unnebrink K, Holz FG. Analysis of digital scanning laser ophthalmoscopy fundus autofluorescence images of geographic atrophy in advanced age-related macular degeneration. Graefe's archive for clinical and experimental ophthalmology = Albrecht von Graefes Archiv fur klinische und experimentelle Ophthalmologie. 2002;240(2):73–78.
42. Schmitz-Valckenberg S, Bindewald-Wittich A, Dolar-Szczasny J, et al.Correlation between the area of increased autofluorescence surrounding geographic atrophy and disease progression in patients with AMD. Investigative ophthalmology & visual science. 2006;47(6):2648–2654. [PubMed: 16723482]
43. Schmitz-Valckenberg S, Fleckenstein M, Gobel AP, Hohman TC, Holz FG. Optical coherence tomography and autofluorescence findings in areas with geographic atrophy due to age-related macular degeneration. Investigative ophthalmology & visual science. 2011;52(1):1–6. [PubMed: 20688734]
44. Brar M, Kozak I, Cheng L, et al.Correlation between spectral-domain optical coherence tomography and fundus autofluorescence at the margins of geographic atrophy. American journal of ophthalmology. 2009;148(3):439–444. [PubMed: 19541290]
45. Khanifar AA, Lederer DE, Ghodasra JH, et al.Comparison of color fundus photographs and fundus autofluorescence images in measuring geographic atrophy area. Retina (Philadelphia, Pa). 2012;32(9):1884–1891.
46. Sayegh RG, Simader C, Scheschy U, et al.A systematic comparison of spectral-domain optical coherence tomography and fundus autofluorescence in patients with geographic atrophy. Ophthalmology. 2011;118(9):1844–1851. [PubMed: 21496928]
47. Fleckenstein M, Schmitz-Valckenberg S, Adrion C, et al.Tracking progression with spectral-domain optical coherence tomography in geographic atrophy caused by age-related macular degeneration. Investigative ophthalmology & visual science. 2010;51(8):3846–3852. [PubMed: 20357194]
48. Guymer RH, Rosenfeld PJ, Curcio CA, et al.Incomplete Retinal Pigment Epithelial and Outer Retinal Atrophy in Age-Related Macular Degeneration: Classification of Atrophy Meeting Report 4. Ophthalmology. 2020;127(3):394–409. [PubMed: 31708275]
49. Wu Z, Luu CD, Ayton LN, et al.Optical coherence tomography-defined changes preceding the development of drusen-associated atrophy in age-related macular degeneration. Ophthalmology. 2014;121(12):2415–2422. [PubMed: 25109931]
50. Wu Z, Luu CD, Hodgson LAB, et al.Prospective Longitudinal Evaluation of Nascent Geographic Atrophy in Age-Related Macular Degeneration. Ophthalmology Retina. 2020;4(6):568–575. [PubMed: 32088159]
51. Waldstein SM, Vogl WD, Bogunovic H, Sadeghipour A, Riedl S, Schmidt-Erfurth U. Characterization of Drusen and Hyperreflective Foci as Biomarkers for Disease Progression in Age-Related Macular Degeneration Using Artificial Intelligence in Optical Coherence Tomography. JAMA ophthalmology. 2020;138(7):740–747. [PubMed: 32379287]
52. Nassisi M, Lei J, Abdelfattah NS, et al.OCT Risk Factors for Development of Late Age-Related Macular Degeneration in the Fellow Eyes of Patients Enrolled in the HARBOR Study. Ophthalmology. 2019;126(12):1667–1674. [PubMed: 31281056]
53. Sleiman K, Veerappan M, Winter KP, et al.Optical Coherence Tomography Predictors of Risk for Progression to Non-Neovascular Atrophic Age-Related Macular Degeneration. Ophthalmology. 2017;124(12):1764–1777. [PubMed: 28847641]

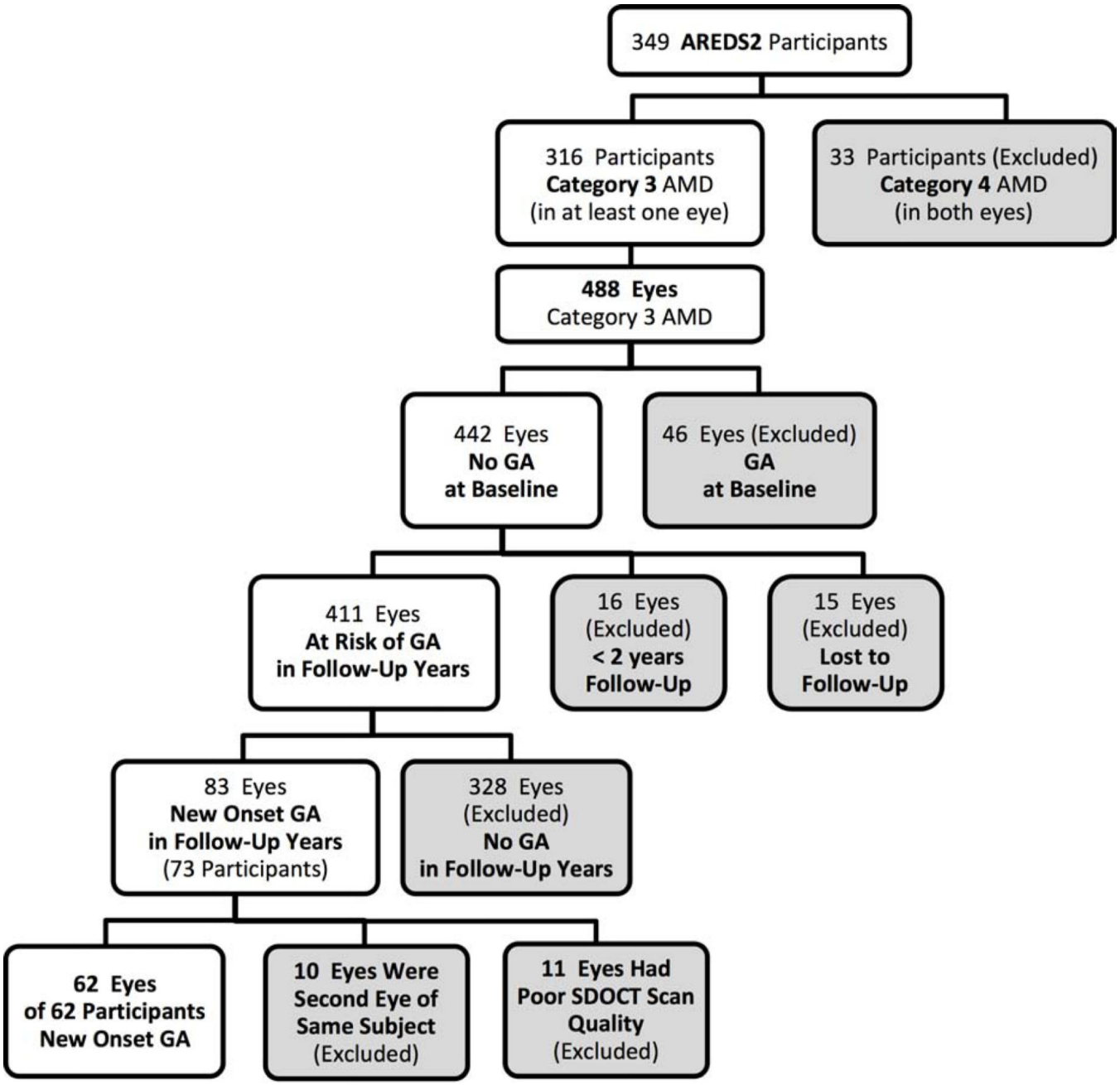

Figure 1.

Flowchart on subset of participants from Age-Related Eye Disease Study 2 (AREDS2) enrolled in the present study. This study included 62 eyes of 62 participants with new onset geographic atrophy (GA).

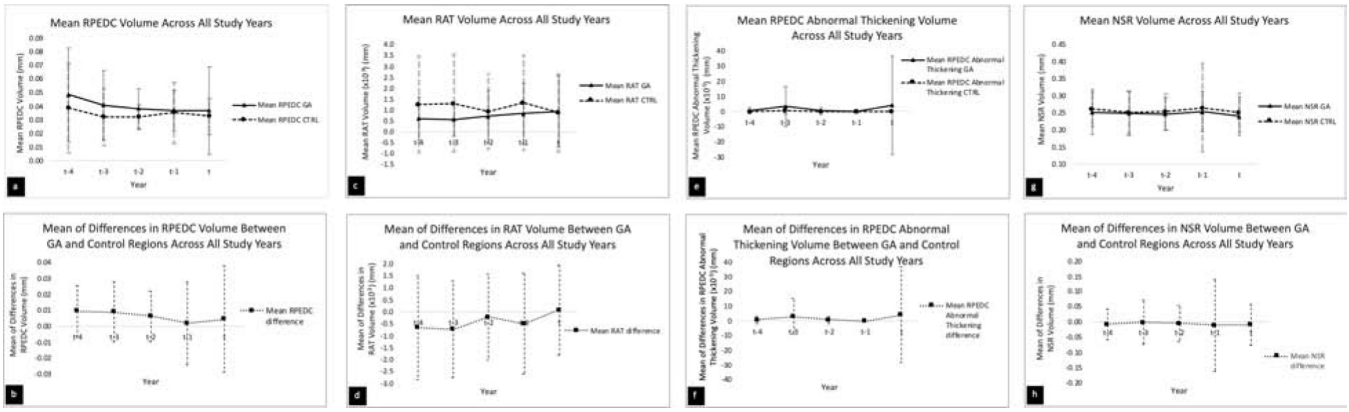

Figure 2.

a-b. Graphical representation of mean and mean of differences between geographic atrophy and control regions (GA – Control) with respect to retinal pigment epithelium drusen complex (RPEDC) volume across all study years.

c-d. Graphical representation of mean and mean of differences between geographic atrophy and control regions with respect to RPEDC abnormal thinning (RAT) volume across all study years.

e-f. Graphical representation of mean and mean of differences between geographic atrophy and control regions with respect to RPEDC Abnormal Thickening volume across all study years.

g-h. Graphical representation of mean and mean of differences between geographic atrophy and control regions with respect to neurosensory retinal (NSR) volume across all study years.

Note: The 2 lines were not statistically compared because the individual values were paired.

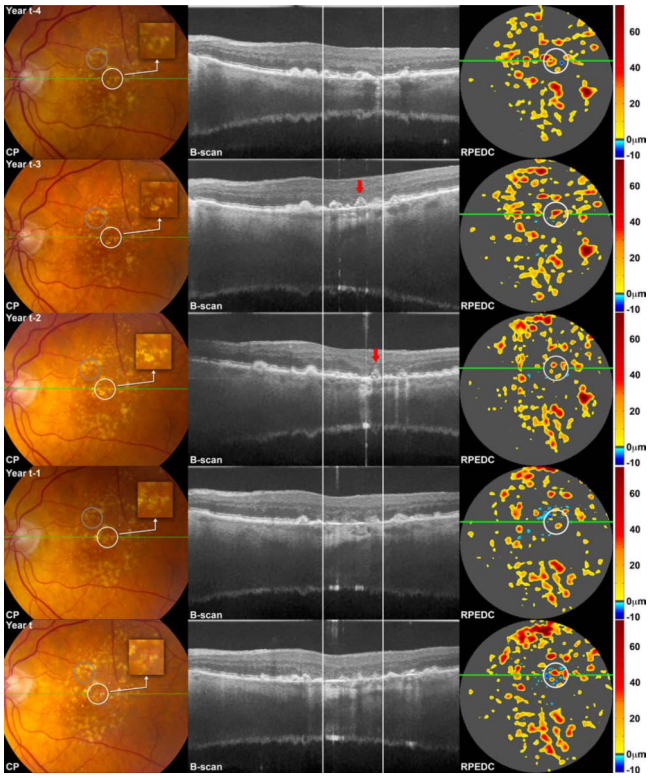

Figure 3.

Color photographs (CP), spectral domain optical coherence tomography (SDOCT) B-scans at the site of the green line on CP, and SDOCT-derived retinal pigment epithelium drusen complex (RPEDC) thickness maps for the 5 mm diameter macular region, at year of new onset geographic atrophy (GA) (**bottom row**) and at one **(first row from bottom)**, two **(second row from bottom)**, three **(third row from bottom)** and four **(fourth row from bottom)** years prior to new onset of GA for a single study eye. On thickness maps, the *dark gray areas* designate RPEDC which is in the normal range of thickness in contrast to *red and orange tones* which designate areas of RPEDC Abnormal Thickening volume and *blue tones* which designate RPEDC Abnormal Thinning (RAT) volume.[12] The region of interest (ROI) containing new onset GA is shown on the CP and SDOCT-derived thickness map at GA incident year (white circles, **bottom row**) and project to the white lines on the B-scan. The white circles in the **rows above** track the locations of this ROI at one, two, three, and four years prior to new onset GA. (The control ROI is shown as a gray circle on the CP in the bottom row and as a tracked location in the rows above; however these ROIs are not projected onto the B-scans or thickness maps). The ROI containing new onset GA correspond to atrophic changes on the CP (increased visibility of choroidal vessels, sharp edges, roughly circular shape, depigmentation), B-scan (loss of photoreceptor zone and RPE, hypertransmission), and thickness map (blue tone). The 3-year, 2-year and 1-year precursor regions correspond to drusen on CP; drusen, progressive thinning/loss of the external limiting membrane, photoreceptor zone, ellipsoid zone, interdigitation zone, and RPE, as well as hypertransmission on B-scan; thickened drusen on the thickness map. The 4-year precursor region is similar on the CP and thickness map; on B-scan, drusen, early thinning/loss of the photoreceptor zone, ellipsoid zone, interdigitation zone, and RPE

is apparent. Note the OCT-reflective drusen substructure (conical debris subtype, indicated with a red arrow) on the 3-year precursor B-scan, which collapses into an atrophic region in the 2-year precursor B scan. Adjacent to this atrophic region on the 2-year precursor B scan, there is a new OCT-reflective drusen substructure (conical debris subtype, also indicated with a red arrow).

Table 1.

Definition of SDOCT-based study outcomes

Outcome[a]	Definition
Continuous Quantitative Outcomes [b]	
Drusen-RPE Combined Volume; RPE Drusen Complex Volume (RPEDC, mm^3)	Drusen-RPE combined volume; Volume between the inner border of the RPE cell bodies and outer border of Bruch's membrane[12]
RPEDC Abnormal Thickening Volume ($x10^{-5}$, mm^3)	Volume of RPEDC abnormal thickening ≥3 SD from the mean of a normative dataset for each pixel location in non-AMD eyes12,13,20
RPEDC Abnormal Thinning Volume (RAT, $x10^{-3}$, mm^3)	Volume of RPEDC abnormal thinning ≤2 SD from the mean of a normative dataset for each pixel location in non-AMD eyes[12,13,20]
Neurosensory Retinal Volume (NSR, mm^3)	Volume between internal limiting membrane and inner border of RPE
Categorical Qualitative Outcomes	
RPE Elevation	Includes both drusen and pigment epithelial detachments
External Limiting Membrane Disruption	External limiting membrane disruption (loss, thinning, distortion, descent) in the presence or absence of other pathologies
Photoreceptor Zone Thinning	Loss of volume of region between inner aspect of the outer plexiform layer and inner border of RPEDC as compared to adjacent tissue; Additionally rank-graded as none (0 = No thinning, 1 = 25% thinning, 2 = 50% thinning, 4= 100% thinning)
Ellipsoid Zone Disruption	Ellipsoid zone disruption (loss, thinning, distortion, descent) in the presence or absence of other pathologies
Interdigitation Zone Disruption	Interdigitation zone disruption (loss, thinning, distortion, descent) in the presence or absence of other pathologies
RPE Layer Loss	A clear degradation of the reflectivity and thickness of the RPE layer with persisting outer retinal layers; Additionally rank-graded as none (0 = Intact, 1 = Disrupted, 2 = Absent)
Hypertransmission	Increased transmission of signal below the level of the RPE and into the choroid resulting from loss of scatter or attenuation from overlying RPE and neurosensory retina CAM3; Additionally rank-graded as none (0 = None, 1 = Moderate, 2 = Complete)
Vitreomacular Traction/Epiretinal Membrane (VMT/ERM)	Vitreomacular traction: Deformation of the retina due to vitreal traction Epiretinal membrane: Visible separation of membranous tissue above the internal limiting membrane with deformation of the macula
Cystoid Spaces	Round or oval hyporeflective areas within the retinal layers, usually nuclear layers
Subretinal Fluid	Area of low reflectivity (less than or comparable to the vitreous gel) between the outer surface of the retina and the retinal pigment epithelium
Subretinal or Intraretinal Lesion	Subretinal hyperreflective material (SHRM), hemorrhage, subretinal drusenoid deposit, vitelliform lesion, retinal angiomatous proliferation (type 3 macular neovascularization)
Hyperreflective Foci (HRF)	Focal, well-circumscribed intraretinal hyperreflective lesions within the neurosensory retina overlying drusen not associated with intraretinal vessels[3]
OCT-reflective Drusen Substructures (ODS)	Low-reflective cores: Focal, well-circumscribed hypo-reflective focus within druse High-reflective cores: Focal, well-circumscribed hyper-reflective focus within druse Conical debris: Conical shaped druse with ≥3 focal, well-circumscribed hyper-reflective cores within Split drusen: Entire druse is split into two subvolumes of low and high reflectivity

[a] Abbreviations: RPE= retinal pigment epithelium, OCT= optical coherence tomography

[b] Continuous= Measured by semi-automated segmentation of retinal layers (previously validated and described by Chiu et al 2012 and 2010)[21,22,23]

Table 2.

A comparison of quantitative and categorical qualitative SDOCT findings between geographic atrophy (GA) precursor regions vs. control regions (one GA precursor region and one control region per eye) in 62 eyes at 2-, 3-, and 4-years prior to the new onset of GA

	4 Year Precursor Regions			3 Year Precursor Regions			2 Year Precursor Regions[†]		
	GA Regions[a]	Control Regions[a]	p-value[b]	GA Regions[a]	Control Regions[a]	p-value[b]	GA Regions[a]	Control Regions[a]	p-value[b]
Number of ROIs[c]	25	25		33	33		54	54	
	Mean (SD)	Mean (SD)		Mean (SD)	Mean (SD)		Mean (SD)	Mean (SD)	
RPE Drusen Complex Volume (mm^3/mm^2)[d]	**0.0482 (0.0342)**	**0.0388 (0.0326)**	**0.0025**	**0.0408 (0.0254)**	**0.0319 (0.0206)**	**0.0033**	**0.0381 (0.0150)**	**0.0320 (0.0091)**	**0.0113**
RPEDC Abnormal Thickening Volume ($x10^{-5}$) (mm^3/mm^2)[d]	**0.5470 (2.363)**	**0.0378 (0.1106)**	**0.0223**	3.2400 (13.2300)	0.3700 (2.1255)	0.0898	0.4940 (2.3168)	0.0129 (0.0933)	0.1766
RPEDC Abnormal Thinning (RAT) Volume ($x10^{-3}$) (mm^3/mm^2)[d]	**0.6000 (0.9912)**	**1.2700 (2.2181)**	**0.0379**	0.5700 (0.7851)	1.3100 (2.2444)	0.1903	0.7100 (1.1886)	0.9400 (1.7260)	0.3787
Neurosensory Retinal Volume (mm^3/mm^2)[d]	0.2519 (0.0645)	0.2602 (0.0487)	0.2497	0.2487 (0.0637)	0.2508 (0.0609)	0.6812	0.2462 (0.0483)	0.2529 (0.0517)	0.2409
	Proportion (%)	Proportion (%)		Proportion (%)	Proportion (%)		Proportion (%)	Proportion (%)	
RPE Elevation	25/25 (100.00)	21/25 (84.00)	-----	**32/33 (96.97)**	**28/33 (84.85)**	**0.0455**	54/54 (100.00)	44/54 (81.48)	-----
External Limiting Membrane Disruption	21/22 (95.45)	18/22 (81.82)	0.0833	**21/22 (95.45)**	**17/22 (77.27)**	**0.0455**	43/45 (95.56)	38/45 (84.44)	0.0588
Photoreceptor Zone Thinning[*]	**12/25 (48.00)**	**3/25 (12.00)**	**0.0027**	**18/33 (54.55)**	**9/33 (27.27)**	**0.0126**	**36/54 (66.67)**	**13/54 (24.07)**	**<0.0001**
Ellipsoid Zone Disruption	22/25 (88.00)	20/25 (80.00)	0.4142	**29/32 (90.63)**	**21/32 (65.63)**	**0.0114**	**53/54 (98.15)**	**42/54 (77.78)**	**0.0009**
Interdigitation Zone Disruption	**24/25 (96.00)**	**20/25 (80.00)**	**0.0455**	31/32 (96.88)	27/32 (84.38)	0.1025	50/50 (100.00)	47/50 (94.00)	-----
RPE Layer Loss[*]	19/25 (76.00)	13/25 (52.00)	0.0833	**27/33 (81.82)**	**14/33 (42.42)**	**0.0046**		**23/54 (42.59)**	**<0.0001**
Hypertransmission[*]	13/25 (52.00)	9/25 (36.00)	0.1573	**16/33 (48.48)**	**8/33 (24.24)**	**0.0325**	**37/54 (68.52)**	**11/54 (20.37)**	**<0.0001**
VMT/ERM	4/25 (16.00)	3/25 (12.00)	0.3173	4/33 (12.12)	1/33 (3.03)	0.0833	**6/54 (11.11)**	**1/54 (1.85)**	**0.0253**
Cystoid Spaces	0/24 (0.00)	0/24 (0.00)	1.00	**8/32 (25.00)**	**2/32 (6.25)**	**0.0339**	3/54 (5.56)	2/54 (3.70)	0.3173
Subretinal Fluid	1/24 (4.17)	0/24 (0.00)	-----	2/33 (6.06)	0/33 (0.00)	-----		0/54 (0.00)	-----
Subretinal Lesion[e]	4/25 (16.00)	5/25 (20.00)	0.6547	6/33 (18.18)	10/33 (30.30)	0.1025	**5/54 (9.26)**	**15/54 (27.78)**	**0.0039**
Hyperreflective Foci	11/25 (44.00)	5/25 (20.00)	0.0578	**14/33 (42.42)**	**6/33 (18.18)**	**0.0455**	**30/54 (55.56)**	**11/54 (20.37)**	**0.0003**

	4 Year Precursor Regions			3 Year Precursor Regions			2 Year Precursor Regions†		
	GA Regions[a]	Control Regions[a]	p-value[b]	GA Regions[a]	Control Regions[a]	p-value[b]	GA Regions[a]	Control Regions[a]	p-value[b]
Number of ROIs[c]	**25**	**25**		**33**	**33**		**54**	**54**	
	Mean (SD)	**Mean (SD)**		**Mean (SD)**	**Mean (SD)**		**Mean (SD)**	**Mean (SD)**	
OCT-reflective Drusen Substructures	4/21 (19.05)	3/21 (14.29)	0.6547	**6/28 (21.43)**	**1/28 (3.57)**	**0.0253**	**14/44 (31.82)**	**2/44 (4.55)**	**0.0027**

†Primary endpoint

*Additionally measured on categorical scales (see Table 4) Yellow highlight indicates significant findings.

[a]GA and Control Regions of Interest (ROIs) were identified at GA incident year.

[b]Wilcoxon Signed Rank and Bowker's tests for matched pairs with alpha value = 0.05; "-" indicates test could not be carried out due to asymmetry. The p-values refer to paired data rather than a comparison of the 2 means reported in the columns to the left of the p-value.

[c]ROIs in each precursor year are a subset of the 62 incident GA ROIs, not a subset of the adjacent precursor year

[d]SDOCT volumes (left column, top section of table) within each ROI were divided by the ROI area to standardize outcomes.

[e]Subretinal Hyperreflective Material (SHRM), Hemorrhage, Subretinal Drusenoid Deposit, Vitelliform Lesion, Retinal Angiomatous Proliferation

Table 3.

Subcategory Breakdown of Selected SDOCT Findings in 2-, 3-, and 4-year Precursor Regions of New Onset Geographic Atrophy

	4 Year Precursor Regions			3 Year Precursor Regions			2 Year Precursor Regions		
	GA Regions[a]	Control Regions[a]	p-value[b]	GA Regions[a]	Control Regions[a]	p-value[b]	GA Regions[a]	Control Regions[a]	p-value[b]
	Proportion (%)	Proportion (%)		Proportion (%)	Proportion (%)		Proportion (%)	Proportion (%)	
Subretinal lesion	4/25 (16.00)	5/25 (20.00)	0.6547	6/33 (18.18)	10/33 (30.30)	0.1025	**5/54 (9.26)**	**15/54 (27.78)**	**0.0039**
a. SHRM	0/4 (0.00)	0/5 (0.00)	-----	1/6 (14.29)	0/10 (0.00)	-----	1/5 (20.00)	1/15 (6.67)	-----
b. Hemorrhage	0/4 (0.00)	0/5 (0.00)	-----	0/6 (0.00)	0/10 (0.00)	-----	1/5 (20.00)	0/15 (0.00)	-----
c. Subretinal Drusenoid Deposit	4/4 (100.00)	5/5 (100.00)	-----	3/6 (42.86)	10/10 (100.00)	-----	4/5 (80.00)	14/15 (93.33)	-----
d. Vitelliform	0/4 (0.00)	0/5 (0.00)	-----	2/6 (28.57)	0/10 (0.00)	-----	0/5 (0.00)	0/15 (0.00)	-----
e. Retinal Angiomatous Proliferation (Type 3 Macular Neovascularization)	0/4 (0.00)	0/5 (0.00)	-----	0/6 (0.00)	0/10 (0.00)	-----	0/5 (0.00)	0/15 (0.00)	-----
RPE Elevation	25/25 (100.00)	21/25 (84.00)	-----	**32/33 (96.97)**	**28/33 (84.85)**	**0.0455**	54/54 (100.00)	44/54 (81.48)	-----
a. Drusen	25/25 (100.00)	21/21 (100.00)	-----	31/32 (96.88)	28/28 (100.00)	-----	54/54 (100.00)	44/44 (100.00)	-----
b. PED	0/25 (0.00)	0/21 (0.00)	-----	4/32 (12.50)	1/28 (3.57)	-----	5/54 (9.26)	1/44 (2.27)	-----
b1. PED fluid component	0/0 (--)	0/0 (--)	-----	1/4 (25.00)	0/1 (0.00)	-----	1/5 (20.00)	0/1 (0.00)	-----

Note: Regions could contain more than one subcategory of features.

[a] GA and Control Regions of Interest (ROIs) were identified at GA incident year.

[b] Wilcoxon Signed Rank and Bowker's tests for matched pairs with alpha value = 0.05; "-" indicates test could not be carried out due to asymmetry. Matched pairs statistical analysis could not be carried out for outcome subcategories due to asymmetrical dataset. The p-values refer to paired data rather than a comparison of the 2 means reported in the columns to the left of the p-value.

Table 4.

Analysis of selected SDOCT findings additionally scored on categorical scales at 2-, 3-, and 4-years prior to new onset of geographic atrophy

	4 Year Precursor Regions		3 Year Precursor Regions		2 Year Precursor Regions	
	GA Regions[a]	Control Regions[a]	GA Regions[a]	Control Regions[a]	GA Regions[a]	Control Regions[a]
Number of ROIs[b]	**25**	**25**	**33**	**33**	**54**	**54**
	% (Number)	**% (Number)**	**% (Number)**	**% (Number)**	**% (Number)**	**% (Number)**
Photoreceptor Zone Thinning [c]						
No thinning = 0	52 (13)	92 (23)	(45) 15	73 (24)	33 (18)	76 (41)
25% thinning = 1	12 (3)	4 (1)	18 (6)	21 (7)	19 (10)	20 (11)
50% thinning = 2	24 (6)	4 (1)	15 (5)	6 (2)	26 (14)	4 (2)
100% thinning = 4	12 (3)	0 (0)	21 (7)	0 (0)	22 (12)	0 (0)
RPE Layer Loss						
Intact = 0	24 (6)	48 (12)	18 (6)	58 (19)	2 (1)	57 (31)
Disrupted = 1	60 (15)	52 (13)	61 (20)	30 (10)	59 (32)	41 (22)
Absent = 2	16 (4)	0 (0)	21 (7)	12 (4)	39 (21)	2 (1)
Hypertransmission						
0% increase =0	48 (12)	64 (16)	52 (17)	76 (25)	31 (17)	80 (43)
50% increase = 1	40 (10)	36 (9)	27 (9)	21 (7)	56 (30)	20 (11)
100% increase = 2	12 (3)	0 (0)	21 (7)	3 (1)	13 (7)	0 (0)

[a] GA and Control Regions of Interest (ROIs) were identified at GA incident year.

[b] ROIs in each precursor year are a subset of the 62 incident GA ROIs, not a subset of the adjacent precursor year

[c] Photoreceptor zone thinning was measured by degree of outer plexiform layer dipping towards the RPE.

Table 5.

A comparison of SDOCT-based retinal volume measurements between geographic atrophy (GA) precursor regions vs. control regions at 1-year prior to and incident year of new onset of GA (post-hoc analysis)

	1 Year Precursor Regions			GA Incident Year Regions		
	GA Regions[a]	Control Regions[a]	p-value[b]	GA Regions[a]	Control Regions[a]	p-value[b]
Number of ROIs[c]	**53**	**53**		**62**	**62**	
	Mean (SD)	**Mean (SD)**		**Mean (SD)**	**Mean (SD)**	
RPE Drusen Complex Volume (mm^3/mm^2) [d]	0.0367 (0.0147)	0.0350 (0.0224)	0.0835	0.0367 (0.0318)	0.0323 (0.0132)	0.8327
RPEDC Abnormal Thickening Volume ($x10^{-5}$) (mm^3/mm^2) [d]	0.0024 (0.0164)	0.1470 (0.8975)	0.9555	4.1644 (32.30)	0.03251 (0.2553)	0.2497
RPEDC Abnormal Thinning (RAT) Volume ($x10^{-3}$) (mm^3/mm^2) [d]	0.8400 (1.4101)	1.340 (2.1619)	0.6340	**0.9316 (1.6295)**	**0.8643 (1.7613)**	**0.0340**
Neurosensory Retinal Volume ($mm3/mm^2$) [d]	0.2532 (0.0591)	0.2648 (0.1279)	0.9756	**0.2403 (0.0564)**	**0.2497 (0.0564)**	**0.0204**

[a] GA and Control Regions of Interest (ROIs) were identified at GA incident year.

[b] Wilcoxon Signed Rank and Bowker's tests for matched pairs with alpha value = 0.05. The p-values refer to paired data rather than a comparison of the 2 means reported in the columns to the left of the p-value.

[c] ROIs in each precursor year are a subset of the 62 incident GA ROIs, not a subset of the adjacent precursor year

[d] SDOCT volumes (left column of table) within each ROI were divided by the ROI area to standardize outcomes.